The Effect of Ionic Strength and pH on the Dewatering Rate of Cellulose Nanofibril Dispersions

Andreas Fall
RISE Avdelning Material- och ytdesign
Marielle Henriksson
RISE Avdelning Material- och ytdesign
Anni Karppinen
Borregaard
Anne Opstad
Borregaard
Ellinor Bævre Heggset
RISE PFI AS
Kristin Syverud (kristin.syverud@rise-pfi.no)
RISE PFI AS https://orcid.org/0000-0003-2271-3637

Research Article

Keywords: Nanocelluloses, cellulose nanofibrils, dewatering, redispersion, rheology

Posted Date: December 22nd, 2021

DOI: https://doi.org/10.21203/rs.3.rs-1156117/v1

Abstract

Cellulose nanofibrils, CNFs, show a great potential in many application areas. One main aspect limiting the use of the material is the slow and energy demanding dewatering of CNF suspensions. Here we investigate the dewatering with a piston press process. Three different CNF qualities, two laboratory grades (high and low charge) and one industrial grade (low charge) were tested. The chemical conditions were varied by changing salt concentration (NaCl) and pH. For the original suspensions, the dewatering rate is substantially slower for the high charge CNFs. However, by changing the conditions it dewatered as fast as the two low charge CNFs, even though salt/acid additions also improved dewatering rate for these two CNFs. Finally, by tuning the conditions fast dewatering could be obtained with only minor effect on strength and barrier performance of films prepared from the CNFs.

Introduction

Nanocelluloses comprise a group of cellulosic materials with dimensions in nanoscale that are hydrophilic, crystalline, stiff, and high aspect ratio fiber-like particles isolated from various natural sources. Their small width (2 to 100 nm) provides a very large specific surface area. Often nanocelluloses are chemically modified to add functionalities by for example introducing ionizable groups (surface charges), which also facilitates isolation of the particles and provides good dispersibility and stability in water. The isolation of nanocellulose particles has allowed for bottom-up formation of many types of materials (e.g. films, foams and fibers) with fascinating properties such as strong and light, transparent and with great gas barrier.

Nanocelluloses have also been used in wet applications. Because dispersions of nanocelluloses are highly viscous and shear thinning different types of nanocelluloses have been studied as rheological modifiers (Herrick et al.1983; Pääkkö et al. 2007; Karppinen et al. 2011; Dimic-Misic et al. 2017; Aaen et al. 2019a; Heggset et al. 2019). Additionally, as fibrillar networks are formed at very low concentrations nanocelluloses have been utilized to disperse several exotic materials in water media by trapping them in the network, e.g. carbon nanotubes (Hajan et al. 2017), graphenes (Yang et al. 2017) and metal organic frameworks MOFs (Zhu et al. 2016).

However, nanocellulose suspensions are hard to dewater, providing tedious and costly drying procedures, which significantly limit the industrial use of nanocelluloses. This is especially true for cellulose nanofibrils (CNFs), which are the focus of this study. As CNFs are hydrophilic, have high aspect ratio, are relatively stiff rod-like particles that produce kinetically arrested networks (gels) at extremely low solid contents, water is strongly held by the CNF networks. In addition, rigid fibrillar CNF networks are created that need to be compressed to remove water from the system. The network strength increases exponentially with the CNF concentration (Naderi et al. 2014a; Aaen et al. 2019a). Finally, the particles are often charged, increasing their hydrophilicity and providing an osmotic driving force holding/absorbing water (Aaen et al. 2019b). All these factors provide a very high water-holding capacity and strength, making it energy demanding and time consuming to dewater CNF suspensions.

For complete isolation and the possibility to form homogenous networks the nanocellulose qualities need to be prepared below the network concentration (Geng et al. 2018; Nordenström et al. 2017; Håkansson 2021). If the starting concentration is too high, particle flocs are formed, resulting in inhomogeneous material distribution and reduction in material properties, e.g. strength of films (Håkansson 2021). Due to the high aspect ratio of CNFs this demands material formation often below 1 wt%, generally between 0.1 to 0.2 wt% (Håkansson 2021), requiring subsequent removal of a lot of water. Removing all this water purely by heat driven evaporation from 0.2 wt% suspension would result in very high cost of drying, exceeding $40 per dry kilogram of CNF. Hence, water needs to be removed by other more energy efficient means to make CNF materials industrial viable.

Vacuum filtration is used in papermaking and applied in academia to dewater CNF suspensions. However, the process is too slow, taking hours for fine qualities of CNFs. In addition, the concentration reached by vacuum dewatering is relatively low, 5–10 wt%. In papermaking wet pressing is often used for dewatering of pulp. Its energy efficiency and rapidness (Unbehend and Britt1982) are intriguing, however, the dewatering time by pressing is substantially increased if CNFs are added to pulp (Rantanen and Maloney 2015). It has been shown to be hard to press pure CNF suspensions. Instead of dewatering the pressing often breaks the CNF gels in fragments or squeezes out the CNF suspension from the press geometry. By using a confined pressing configuration Wetterling et al. (2017) was able to dewater suspensions of the larger sized non-charged microcrystalline cellulose (MCC) particles, and later suspensions of charged cellulose nanocrystals (CNCs) (Wetterling et al. 2018). A constant mechanical pressure of 3 bars was used and the effect of the chemical environment (ionic strength and pH) and the application of an electrical field were investigated. The dewatering of the pure MCC suspension was slow (0.2–1 mL/min, faster in the beginning, slower towards the end), but changing the environment or applying an electrical field increased the rate by more than an order of magnitude. Combining the two further increased the rate, but at the cost of a higher energy demand. The addition of ions resulted in a higher voltage for the same electrical field. Dewatering of CNC suspensions were facilitated in a similar manner. Similar trends are expected for CNF suspensions.

Dimic-Misic et al. (2013a) combined rheology measurements with vacuum filtering to better understand why CNF suspensions are so slow to dewater. High and low charged CNFs were compared. The former was substantially slower, even though the rheological properties (viscosity and storage modulus) were lower and less affected by the dewatering. The higher homogeneity in combination with the smaller size of the finer CNFs was suggested to be the prime reason for these effects. In another study by Dimic-Misic et al. (2013b), oscillatory and rotational shear was altered during dewatering of furnishes including nanocellulose. It was argued that this altering may induce a restructuring of the particles favoring dewatering. These new insights are intriguing. Still, more knowledge is needed on how dewatering can be facilitated by chemical and structural changes without hampering decisive properties of the final material.

From the CNF producers' point of view, excessive amounts of water in CNF suspensions increase the shipment cost. Thus, concentrated suspensions are preferred for shipment which then can be redispersed

with preserved properties by the receiver. CNCs can even be dried with good redispersibility if charged and dried with a metal counterion (Beck et al. 2012). However, most CNFs irreversibly aggregate during drying, causing loss in properties. Their higher aspect ratio leads to increased particle interactions/entanglements, rendering clustered suspensions upon redispersion. Additives have been shown to improve redispersibility, for example: NaCl (Missoum et al. 2012), glycols (Herrick 1984; Schnell and Jensen 2007), and polysaccharides (Herrick 1984; Häggblom and Vuorenpalo 2014; Beaumont et al. 2017). But these additives are often unwanted in the final products and, thus, an extra cleaning step is needed for its use. Hence, concentrated suspensions are the current preferred alternative for shipment and storage. However, if they are concentrated too much the redispersibility is reduced. Ding et al. (2019) studied redispersibilty of both CNC and CNF suspensions as a function of solid content (up to 65 wt%). The CNFs were TEMPO oxidized which is similar to the carboxymethylated CNFs in our study. Reduced redispersibility was found for all samples concentrated above 20 wt%, which was argued to be due to hornification. From AFM images they saw a clear increase in particle size with increasing solid content. This was confirmed by a correlating reduction in accessible hydroxyl groups assessed by using fluorescent labeling of the nanocelluloses.

In this study we have investigated the dewatering of CNF suspensions from 1 wt% to about 20–30 wt%. Three different qualities were investigated: enzymatic pre-treated (low-charge), carboxymethylated (high-charged), and an industrial grade (low-charge). The chemical environment was changed by adding different levels of salt (NaCl) or acid (HCl). The main objective has been to study the dewatering rate and correlating it to the suspension properties of the different samples. The aim was to facilitate dewatering without hampering suspension and material properties of the different CNF qualities.

Materials And Methods

The laboratory grade CNFs were prepared by fibrillation of softwood sulphite dissolving pulp (Domsjö Dissolving plus, Domsjö Fabriker, Sweden). Two different pretreatments were applied to the pulp prior to fibrillation; enzymatically pretreatment (Päkkäö et al. 2007; Henriksson et al. 2007) and carboxymethylation (Wågberg et al. 2008) with modifications described by Naderi et al. (2016a, b), respectively.

Enzymatically (Enz) pretreatment was done, using 2.5 L phosphate buffer (pH=7). To produce the Enz CNF the treated pulp was microfluidized (M-110EH, Microfluidics Corp., USA) at 2%, passed 1 time at 1700 bar through two Z shaped chambers in series with diameters of 200 and 100 µm. The charge of Enz CNF produced from this pulp is typically around 30 µeq/g. The carboxymethylated (Carb) pulp was microfluidized as previously described for Enz CNF. The charge of Carb CNF was 604 µeq/g, determined by conductimetric titration on the pulp. The industrial grade CNF (Ind CNF) was Exilva provided by Borregaard, Norway. It was delivered at 10 wt% solid content and dispersed using deionized water to 2 wt% solid content according to instructions from the manufacturer.

Analytical grades of NaCl and HCl were purchased from VWR.

Table 1
CNF suspensions with alternation of salt concentration and pH. Enz = enzymatically pretreated CNFs, Carb = carboxymethylated CNFs, Ind = industrial quality, i.e. Exilva from Borregaard.

CNF System	Kind of CNF	Salt concentration (mM)	pH
Enz CNF	Enzymatically pretreated	0	7
Enz CNF 10 mM NaCl	Enzymatically pretreated	10	7
Enz CNF 100 mM NaCl	Enzymatically pretreated	100	7
Enz CNF pH 3	Enzymatically pretreated	0	3
Enz CNF pH 5	Enzymatically pretreated	0	5
Carb CNF	Carboxymethylated	0	7
Carb CNF 10 mM NaCl	Carboxymethylated	10	7
Carb CNF 100 mM NaCl	Carboxymethylated	100	7
Carb CNF pH 3	Carboxymethylated	0	3
Carb CNF pH 5	Carboxymethylated	0	5
Ind CNF	Industrial	0	5
Ind CNF 10 mM NaCl	Industrial	10	5
Ind CNF pH 3	Industrial	0	3

Alteration of salt concentration and pH

The original 2 wt% CNF suspensions were diluted with deionized water to 1 wt%. For the samples with adjusted chemical environment salt or acid was added using 1M NaCl or 1M HCl solutions, respectively. The pure CNF samples was only diluted with deionized water. After adjustments/dilution the samples was passed once through the microfluidizer at 400 bar. Hence, all samples were homogenised equal number of times. Overview of the CNF suspensions is given in Table 1.

The pH of the pure suspensions was 7 for Carb and Enz CNF and pH 5.3 for Ind CNF.

The conductivity was measured on 1 wt% suspensions before and after dewatering and redispersion. The ion conductivity of 100 mM NaCl suspensions was reduced by 88-92% by the dewatering and redispersion. Dewatering

A piston-press with filter paper (Munktell 00H) was used for the dewatering. 91 g of the CNF dispersions with 1 wt% dry content was used per test. The dewatering was carried out according to the following pressure profile: 0.5 bar for 30 min, 1 bar for 30 min, 2 bar for 30 min, 4 bar for 30 min, and 6 bar for 30 min. The pressure gradient was crucial in order to avoid squeezing out CNF suspension from the press

geometry. Due to low dewatering rate, the systems Carb CNF, Carb CNF 10 mM, and Carb CNF pH 5 were kept at 6 bar for 15-17 h (overnight) in order to reach equilibrium. The mass of the released water (filtrate) was recorded continuously and used for calculation of the dewatering rate, which was calculated as the slope between 10 and 30% mass loss. Each experiment was run in triplicate. The final weight of the filter cakes was used to calculate the final dry content. The curves presented are the average of the three batches for each CNF system.

Re-dispersion

The dewatered CNF filter cakes, 3 for each sample type, were immersed in water over night. After immersion the samples were propeller mixed for 2 min at 2000 rpm and thereafter mixed with Polytron for 30 s at 20 000 rpm. The final CNF concentration was 1 wt%.

Structure characterization

The samples were characterized using Atomic Force Microscopy (AFM) and ultraviolet–visible (UV-Vis) spectroscopy and by measurement of the nanofraction before and after redispersion.

AFM

The microscopic features of the samples were studied by AFM, using a Bruker Multimode V AFM equipped with a Nanoscope V Controller (Veeco Instruments Inc., Santa Barbara, CA, USA). The instrument was located at the NorFab facility NTNU Nanolab in Trondheim, Norway. When analyzing the suspensions, 25 µL of the solution (concentration of 0.1 wt%) was placed on freshly cleaved 10 mm mica (Agar Scientific Ltd., Essex, UK), and dried using compressed nitrogen gas (N_2) before imaging. Images were obtained by ScanAsyst mode in air at ambient conditions, with silicon nitride ScanAsyst-air AFM tips (Nom. Spring constant=0.4 $N*m^{-1}$, resonance frequency= 70kHz), Bruker AFM Probes (Bruker Nano Inc., Camarillo, CA, USA). The surface roughness was calculated using the NanoScopeAnalysis software, version 1.5.

Ultraviolet–visible (UV-Vis) spectroscopy

The change in transmittance for the CNF dispersions before and after dewatering and redispersion was studied using a UV-vis Spectrophotometer (UV-1800, Shimadzu, Tokyo, Japan). The samples were diluted to a concentration of 0.08 wt% and mixed properly using a IKA T18 Digital Ultra-Turrax at 4200 rpm for 7 min. Subsequently, the transmittance was measured at a wavelength of 500 nm using a cell path length of 1 cm and a slit width of 2.0 nm. Four parallels were measured for each sample.

Nanofraction measurement

The nanofraction was measured as the relative amount of material which do not sediment during centrifugation at 1000g for 15 min at a consistency of 0.02 wt% of CNFs (Naderi et al. 2014b).

Rheology measurements

Rheology measurements were performed on 1 wt% CNF suspensions using a Kinexus stress-controlled rotational rheometer (Malvern Instruments, Malvern, UK) following previously reported protocol (Naderi et al. 2016a) with an integration time between measuring points of 30 s.

Preparation and evaluation of CNF films

Vacuum filtrated films were prepared, tensile strength and oxygen permeability were evaluated following previously reported protocols (Naderi et al. 2016a). The permeability measurements were conducted at 23°C and 50% RH.

Results And Discussion

Suspension properties and particle structure

The particle structure and rheological properties of the suspensions were characterized, and they are summarized in Figure 1. The three types of CNFs are clearly different. Carb CNF is the most fibrillated showing a finer structure in the AFM image (Figure 1Ai) and higher transmittance, nanofraction, and viscosity (Figure 1B–D). The AFM image of Enz CNF (Figure 1Aii) shows coarsest structure. It also has low nanofraction and the lowest transmittance and viscosity (Figure 1B–D) of all the three CNFs, indicating the lowest degree of fibrillation. The AFM image of Ind CNF (Figure 1Aiii) show finer and more homogenous particle structure than Enz CNF, but still clearly larger than Carb CNF. Similarly, its transmittance and viscosity are in between the other two CNF qualities (Figure 1C&D). The effect of changing the chemical environment, i.e. reducing the electrostatic repulsion, was investigated by adding salt or acid. The properties of Enz CNF do not change much by the additions. The viscosity and the transmittance are only slightly affected (Figure 1C&D, solid blue bars). The changes in ionic strength and pH have larger effect on the viscosity of Ind CNF (Figure 1D, black solid bars)), however, the transmittance stays unaffected (Figure 1C). The largest effect, as expected, is observed for Carb CNF. It is highly charged and changes in ionic strength and pH affects the charge interactions. Both addition of salt and acid to the Carb CNF suspensions reduce the viscosity (Figure 1D, red solid bars), with largest reduction at 100 mM NaCl and pH 3, while the transmittance reduces the most at pH 3 (Figure 1C). All this indicates aggregation of Carb CNF at 100 mM NaCl and at pH 3, which is in accordance with the literature (Fall et al. 2011).

Dewatering

In the dewatering experiments the different CNF suspensions were dewatered in the piston press device, with stepwise increased pressure from 0.5 to 6 bar (Figure 2A). The pure suspensions release water very differently (Figure 2A, solid lines). Dewatering of Carb CNF is substantially slower than that of the two low charged CNFs (Enz and Ind CNF). The Carb CNF has not reached equilibrium even after 19 h of dewatering whereas equilibrium is reached in approximately 2 h for the others. An explanation suggested in the literature is formation of a dense, strong homogenous gel of fine fibrillar structure (Dimic-Misic et

al. 2013b). In addition, the high charge of the material makes it more hydrophilic and osmotically prone to swell and hold water.

The effects on the dewatering rate after altering pH or adding NaCl shown in Figure 2A (dotted lines) and the results for all the samples are summarized in Figure 2B. Changing the chemical environment can have a substantial effect on the dewatering rate, especially when largely changed. At pH 3 all three types of CNFs dewater considerably faster, as well as at 100 mM NaCl for Carb and Enz CNF (not measured for Ind CNF). Under these conditions the electrostatic effects are to a large extent cancelled out. The surface charge is drastically reduced at pH 3 (Fall et al. 2011), as pKa of carboxylic groups attached to cellulose are around 4.8 (Lindgren and Öhman 2000), and at 100 mM NaCl most of the charges are screened (Fall et al. 2011). Hence, as the charge interactions are cancelled out it is logical that the high charge CNFs start to behave as the two low charged CNFs. Both Carb and Enz CNFs are expected to aggregate at these conditions (Fall et al. 2011), and most likely also Ind CNF as it is expected to behave similar to Enz CNF. Aggregation would create larger structures and, thus, most likely larger spaces between these structures. The larger spaces may act as channels for water transport, hence increasing the permeability of the network. The network strength may also reduce, as aggregation will lead to reduction in aspect ratio and thus fewer connections between the structures of the network, making it less demanding to compress the network. Both these aspects should facilitate dewatering.

At more moderate changes (pH 5 and 10 mM), dewatering rate is increased for the low charged CNFs whereas it is unaffected for Carb CNF (Figure 2B). Under these conditions Carb CNF still has a significant electrostatic repulsion. The smaller changes in transmittance and viscosity (Figure 1C&D) indicates lower degree of particle aggregation. Thus, the effects on permeability and on network strength are expected to be low. The increase in dewatering rate is especially large for Enz CNF. The rate is more increased at 10 mM NaCl but also increases significantly at pH 5. At these conditions the viscosity of Enz CNF is barely affected, indicating little effect on its structure. Thus, the increased dewatering rate for Enz CNF may be more a chemical (osmotic) effect, as discussed below. For the other low charge CNFs (Ind CNF), however, the viscosity significantly reduces. Thus, aggregation may explain its increased dewatering rate at 10 mM NaCl.

The addition of salt and acid will also reduce osmotic driven counter force for releasing water from the CNF suspensions. If the ion concentration of the released water is significantly lower than the ion concentration of the CNF suspension, which includes both the added ions and the counterions associated to the CNFs, an osmotic force will be generated to hold the water within CNF network. Note that the counterions associated to CNFs surface charges will not be released during the dewatering. For the original suspensions pure water will be released and the strongest osmotic force will be generated, which will be stronger for the higher charged Carb CNF, as it has more counterions. The counterion concentration at 1 wt% for Carb CNF is about 6 mM and for the lower charged CNFs around 0.5 mM. If the added salt concentration is significantly higher than these concentrations the osmotic force will be cancelled out. In addition, reducing the pH will protonate the carboxylic charges and, thus, release counterions, further reducing the osmotic force. As the dewatering rate of Enz CNF is significantly

increased at 10 mM NaCl and at pH 5, where the viscosity is barely affected, the reduction in the osmotic force may be an important factor. For Ind CNF the effect on the osmotic force is expected to be similar, but, as the viscosity also is reduced, the increased dewatering rate is expected to be a combination between the chemical (osmotic) and the structure (viscosity) changes. For Carb CNF it may also be a combination. The higher charge provides lower reduction in the osmotic force at low additions of salt and acid, where also low effects on the viscosity is observed. At pH 3 the structure is largely affected by reduction in nanofraction, transmittance and viscosity, but the osmotic force is also reduced. At 100 mM NaCl though, the reduction in the osmotic force may be more profound for the increased dewatering rate, as the structure of Carb CNF is less affected, seen from the small reduction in nanofraction and transmittance but still the sample has large reduction in viscosity.

As the osmotic force is hard to measure or estimate, the parameter that shows the best correlation with the dewatering rate in our study is the viscosity, i.e. faster dewatering with lower viscosity (Figure 3). It appears to be a threshold in viscosity, above no effect is found but below it has a large impact. This threshold may be related to the specific dewatering setup and procedure used in the study. The figure shows that the coarser qualities of this study, Enz and Ind CNF, follow a similar trajectory whereas the more fibrillated Carb CNF has its own trajectory. This is reasonable as Carb CNF differs, both chemically and structurally, from the two other CNFs.

When salt and acid are added, the initial viscosity drops, and faster dewatering is observed (Figure 3). However, many other properties of the suspensions will be affected as well, some that might be decisive for rapid dewatering. Dewatering is a complicated phenomenon. It is affected by the hydraulic permeability and the viscoelasticity of the particle network (Hubbe and Heitmann 2007). The viscosity before dewatering describes indirectly how fine the fibrillar structure is. It has been shown that if the fine particles are fractionated out from a CNF suspension, by filtration followed by centrifugation, this fraction provides an almost 10-fold increase in rheological properties, when measured and compared at same solid content as the original non-fractionated suspension (Larsson et al. 2019; Ciftci et al. 2020). The studies used similar CNFs to the Ind CNF in our study. Our results also show significantly higher viscosity for the finer Carb CNF. The suspension’s permeability is crucial for how fast it dewaters. The structure of fines is strongly related to the systems permeability (finer structures, lower permeability), which probably is an important factor for the strong correlation between the viscosity and the dewatering rate.

The final dry content is shown in Table 2. It seems easier to remove larger amount of water from the coarser CNF qualities Enz and Ind compared to the finer Carb CNF, as they reach a higher final dry content. The larger particle structures of Enz and Ind CNF compared to Carb CNF are expected to generate networks of higher hydraulic permeability, potentially explaining their higher final solid content. In most cases Enz CNF reaches a lower final solid content than Ind CNF. This may be explained by its more heterogeneous structure size indicated by the AFM image (Figure 1A). The smaller particles may penetrate the network structure generated by the larger particles and plug channels. Similarly, in papermaking smaller fines can plug the channels created by larger pulp fibers (Hubbe and Heitmann 2007). When salt and acid is added, a lower final solid content is reached for the coarser CNF qualities,

but a higher for Carb CNF, especially at pH 3. The additions will cause the particle–particle interactions to go from repulsive to more and more attractive and eventually cause particle aggregation (Fall et al. 2011), but it may also create stronger fibrillar networks (Saito et al. 2011) if the aggregation is limited. As we in this study homogenize the suspensions after the salt/acid additions, increased structure size by aggregation is promoted. The large drop in transmittance and viscosity for Carb CNF indicates formation of larger structures. This provides fewer contacts between aggregated CNFs and is expected to reduce the network strength. For the other two CNFs the structure size is less effected and the stronger particle–particle interactions may instead create stronger particle networks. This would potentially explain why the additions provide higher final solid content for Carb CNF and a lower for the other two CNFs.

To conclude, altering the chemical environment is very powerful for increasing the dewatering rate, but it comes with a cost of lower final dry content for the coarser CNFs whereas for Carb CNF both the rate and the final dry content is increased.

Table 2
Dry content at the end of dewatering (starting dry content 1 wt%).

CNF System	Final dry content (% (w/w))
Enz CNF	28
Enz CNF 10 mM NaCl	23
Enz CNF 100 mM NaCl	21
Enz CNF pH 3	23
Enz CNF pH 5	32
Carb CNF	15*
Carb CNF 10 mM NaCl	17*
Carb CNF 100 mM NaCl	16
Carb CNF pH 3	21
Carb CNF pH 5	17*
Ind CNF	33
Ind CNF 10 mM NaCl	30
Ind CNF pH 3	25
*Kept at 6 bar for 15-17 h (overnight)	

Effect of dewatering on suspension properties

Figure 4A and B shows the relative change in the suspension properties transmittance and viscosity after dewatering and redispersion. Both the original suspensions and the ones with added salt or acid are

plotted. The relative values are calculated by normalizing the values with the properties of the original suspensions before dewatering. The three different CNFs are affected differently. Carb CNF is the most sensitive. However, at neutral conditions it redisperse very well, and the relative properties are close to 1. The redispersion is also good at the colloidal stable conditions (10 mM NaCl and pH5), with only marginal reduction in the relative properties. However, once Carb CNF aggregates (100 mM NaCl and pH 3) the relative properties are significantly reduced, especially for pH 3. In the case of 100 mM NaCl, the drop is less pronounced for the relative transmittance. Comparing Enz CNF to Carb CNF, the original suspension of Enz CNF is more sensitive to dewatering, but no further reduction is seen by the addition of salt or acid. Changes in chemical environment also marginally affect the relative properties of Ind CNF, but it redisperses slightly better than Enz CNF. Besides the chemical condition of the suspensions, the final dry content may also affect the redispersibility. Ding et al. (2019) showed that above 20 wt% nanocellulose suspensions start to hornify, causing irreversible structure formation which reduces suspension redispersability. Enz and Ind CNF are generally dewatered to a higher final dry content than Carb CNF, which, by hornification may explain their poorer redispersibility. The lower relative transmittance of Carb CNF pH 3 versus Carb CNF 100 mM may also be explained by the higher solid content after dewatering at pH 3, 16 wt% and 21 wt%, respectively. In addition, the nanofraction of redispersed Carb CNF suspensions was measured (not shown). Also, the nanofraction is much higher for the redispersed 100 mM NaCl Carb CNF suspension compared to the redispersed pH3 (56% compared to 22%).

Vacuum filtrated films were prepared from the different CNF systems before and after dewatering and redispersion and evaluated with respect to mechanical properties and oxygen barrier (Figure 4C and D). In general, comparing films from the original suspensions, Carb CNF have better properties than Enz and Ind CNF. This is in line with previous observations (Henriksson et al. 2008; Naderi et al. 2017). Comparing Enz and Ind CNF films, the barrier is better (i.e. lower permeability) for the former and the tensile strength is higher for the latter. Dewatering and redispersion has little effect on the mechanical properties for all original CNFs. Addition of salt and acid affects Carb CNF the most, with reduction in film strength and barrier performance. However, the dewatering removes parts of the added salt and acid, and the redispersed suspensions provide films with lower reduction in strength. This effect is especially pronounced for Carb CNF 100 mM, where redispersion significantly increases the film strength. The NaCl concentration after redispersion is calculated to approx. 5 mM. At this ionic strength Carb CNF is expected to be in a colloidal stable state during the film formation, which may be more important than that the particles still are aggregated as indicated by the low relative transmittance and viscosity, Figure 4A and B. At pH 3 Carb CNF shows a large drop in film strength. This was also observed by Benitez and Walther (2017), where 50% reduction was reported, larger than the 20% reduction in our study. For this suspension the redispersion only provided a minor, non-significant, improvement in strength. However, barrier is generally affected negatively by redispersion (Figure 4D). If salt or acid is added it also provides higher permeability for Carb and Ind CNF, whereas Enz CNF is little effected. The most negative effect has the adjustment to pH 3, doubling the permeability of Carb and Ind CNF films compared to films from the original suspensions.

Conclusions

Dewatering of CNF suspensions was studied by using a piston press setup for three different types of CNFs, two coarser qualities, i.e. one enzymatic pretreated grade and one industrial grade (Enz CNF and Ind CNF), and one finer and highly charged grade, i.e. pretreated using carboxymethylation (Carb CNF). The dewatering rates were substantially increased by altering ionic strength and pH. The most drastic effect was observed when either 100mM NaCl was added or when the pH was adjusted from 7 to 3. In both cases the time after which no more water was possible to press out of the gel dropped from 19 h to less than 1 h for Carb CNF. Under these conditions the Carb CNF releases water equally fast as the coarser CNFs, even though they also were substantially faster to dewater at these conditions. The viscosity before dewatering seemed to provide a good qualitative estimate of the dewatering rate, where lower viscosity gave faster dewatering. Different types of CNFs had different trajectories when plotting dewatering rate against viscosity, but the general trend of increasing rate with decreasing viscosity was the same for all three CNFs. For the coarser CNF qualities (Enz and Ind) the dewatering stopped at a higher final dry content compared to Carb CNF (28 and 33 wt% compared with 15 wt%). Changing ionic strength or pH decreased the final dry content for the coarser CNFs whereas it increased for Carb CNF.

Suspension properties and properties of films prepared from the CNFs were evaluated after dewatering and redispersion. Enz CNF was very robust to these treatments preserving both suspension (transmittance and viscosity) and material properties measured on vacuum filtered films (mechanical and barrier). Ind CNF was slightly more affected, whereas Carb CNF was highly affected with reduction in both suspension and material properties, especially after adjusting to pH 3. This condition provided the fastest dewatering but the reduction in properties is unfortunate. However, the alteration to 100 mM NaCl almost provides as fast water removal with much lower reduction in properties for Carb CNF, especially for films produced from redispersed suspensions. For the coarser lower charged Enz and Ind CNFs the fast dewatering rate at pH 3 could be fully utilized as it only provided minor reduction in properties, actually better properties than when NaCl was added. To conclude, the dewatering of CNF suspensions can be drastically improved by adjusting the suspensions pH or ionic strength, and the adjustment can be made so that the effect on suspension and film properties are limited.

Declarations

Acknowledgements

Åsa Engström, Alice Landmér, AnneMarie Runebjörk (RISE) are acknowledged for carrying out the laboratory work, Birgitte H. McDonagh (RISE PFI) for performing the AFM characterization, Eva Kvernes Rygg for assistance with the TOC figure and Tom Lindström for valuable discussions during the initiation of this study.

Funding

This work was a part of the project NanoVisc: “Development of high-performance viscosifiers and texture ingredients for industrial applications based on Cellulose Nanofibrils (CNF)” financed by the Research Council of Norway through the Nano2021 programme (Grant no. 245300), and the companies Borregaard, Mercer, and Stora Enso. Part of the work has also been funded through the project NanoPlasma: Nanofibril production using plasma (Grant no. 274975) and from RISE.

Competing interests

All the authors declare no conflicts of interest

Authors' contributions

Andreas Fall, Marielle Henriksson, Ellinor Heggset and Kristin Syverud: Study conception and design, material preparation, data collection and analysis, writing and revision of the manuscript.

Anni Karppinen and Anne Opstad: Revision of the manuscript.

All authors read and approved the final manuscript.

References

1. Aaen R, Simon S, Brodin FW, Syverud K (2019a) The potential of TEMPO-oxidized cellulose nanofibrils as rheology modifiers in food systems. Cellulose 26, 5483–5496. https://doi.org/10.1007/s10570-019-02448-3
2. Aaen R, Brodin FW, Simon S, Heggset EB, Syverud K (2019b) Oil-in-Water Emulsions Stabilized by Cellulose Nanofibrils - The Effects of Ionic Strength and pH. Nanomaterials 9:259-272. https://doi.org/10.3390/nano9020259
3. Beaumont M, Konig J, Opietnik M, Potthast A, Rosenau T (2017) Drying of a cellulose II gel: effect of physical modification and redispersibility in water. Cellulose 24:1199-1209. https://doi.org/10.1007/s10570-016-1166-9
4. Beck S, Bouchard J, Berry R (2012) Dispersibility in Water of Dried Nanocrystalline Cellulose. Biomacromolecules 13: 1486-1494. https://doi.org/10.1021/bm300191k
5. Benitez AJ, Walther A (2017) Counterion Size and Nature Control Structural and Mechanical Response in Cellulose Nanofibril Nanopapers, Biomacromolecules 18: 1642–1653. https://doi.org/10.1021/acs.biomac.7b00263
6. Ciftci GC, Larsson PA, Riazanova AV, Øvrebø HH, Wågberg L, Berglund LA (2020) Tailoring of rheological properties and structural polydispersity effects in microfibrillated cellulose suspensions. Cellulose 27: 9227–9241. https://doi.org/10.1007/s10570-020-03438-6
7. Dimic-Misic K, Puisto A, Gane P, Nieminen K, Alava M, Paltakari J, Maloney T (2013a) The role of MFC/NFC swelling in the rheological behavior and dewatering of high consistency furnishes. Cellulose 20:2847-2861. https://doi.org/10.1007/s10570-013-0076-3

8. Dimic-Misic K, Puisto A, Paltakari J, Alava M, Maloney T (2013b) The influence of shear on the dewatering of high consistency nanofibrillated cellulose furnishes. Cellulose 20:1853–1864. https://doi.org/10.1007/s10570-013-9964-9
9. Dimic-Misic K, Maloney T, Liu G, Gane P (2017) Micro nanofibrillated cellulose (MNFC) gel dewatering induced at ultralow-shear in presence of added colloidally-unstable particles. Cellulose 24:1463-1481. https://doi.org/10.1007/s10570-016-1181-x
10. Ding Q, Zwng J, Wang B, Tang D, Chen K, Gao W (2019) Effect of nanocellulose fiber hornification on water fraction characteristics and hydrogen accessibility during dehydration. Carbohydr. Pol. 207:44-51. https://doi.org/10.1016/j.carbpol.2018.11.075
11. Fall A, Lindström S, Sundman O, Ödberg L, Wågberg L (2011) Colloidal Stability of Aqueous Nanofibrillated Cellulose Dispersions. Langmuir 27(18):11332–11338. https://doi.org/10.1021/la201947x
12. Geng L, Mittal N, Zhan C, Ansari F, Sharma PR, Peng X, Hsiao BS, Söderberg DL (2018) Understanding the Mechanistic Behavior of Highly Charged Cellulose Nanofibers in Aqueous Systems. Macromolecules, 51: 1498-1506. https://doi.org/10.1021/acs.macromol.7b02642
13. Hajan A, Lindström BS, Petterson T, Hamedi MM, Wågberg L (2017) Understanding the Dispersive Action of Nanocellulose for Carbon Nanomaterials. Nano Lett. 17:1439–1447. https://doi.org/10.1021/acs.nanolett.6b04405
14. Heggset EB, Strand BL, Sundby KW, Simon S, Chinga-Carrasco G, Syverud K (2019) Viscoelastic properties of nanocellulose based inks for 3D printing and mechanical properties of CNF/alginate biocomposite gels. Cellulose 26:581–595. https://doi.org/10.1007/s10570-018-2142-3.
15. Henriksson M, Henriksson G, Berglund L, Lindström T (2007) An environmentally friendly method for enzyme-assisted preparation of microfibrillated cellulose (MFC) nanofibers. Eur. Polym. J. 43:3434–3441. https://doi.org/10.1016/j.eurpolymj.2007.05.038
16. Henriksson M, Berglund LA, Isaksson P, Lindström T, Nishino T (2008) Cellulose nanopaper structure of high toughness. Biomacromolecules 9:1579-1585. https://doi.org/10.1021/bm800038n
17. Herrick FW, Casebier RL, Hamilton JK, Sandberg KR (1983) Microfibrillated cellulose: morphology and accessibility. J. Appl. Polym. Sci. Appl. Polym. Symp. 37:797–813.
18. Hubbe MA and Heitmann JA (2007) Review of factors affecting the release of water from cellulosic fibers during paper manufacture. Bioresources 2:500–533.
19. Håkansson KMO (2021) Effect of carboxymethylated cellulose nanofibril concentration regime upon material forming on mechanical properties in films and filaments. Cellulose 28:881–895. https://doi.org/10.1007/s10570-020-03566-z
20. Häggblom M, Vuorenpalo VM (2014). "Method for producing dewatered microfibrillated cellulose." Patent number WO 2014/096547.
21. Karppinen A, Vesterinen AH, Saarinen T, Pietikäinen P, Seppälä J (2011) Effect of cationic polymethacrylates on the rheology and flocculation of microfibrillated cellulose. Cellulose 18:1381–1390. https://doi.org/10.1007/s10570-011-9597-9

22. Larsson PA, Riazanova AV, Ciftci GC, Rojas R, Øvrebø HH, Wågberg L, Berglund LA (2019) Towards optimised size distribution in commercial microfibrillated cellulose: a fractionation approach. Cellulose 26: 1565–1575. https://doi.org/10.1007/s10570-018-2214-4
23. Lindgren J, Öhman, LO (2000) Characterization of acid/base properties for bleached softwood fibers as influenced by ionic salt medium Nordic Pulp & Paper Research Journal, 15: 18–23. https://doi.org/10.3183/npprj-2000-15-01-p018-023
24. Missoum K, Bras J, Belgacem, MN (2012) Water Redispersible Dried Nanofibrillated Cellulose by Adding Sodium Chloride. Biomacromolecules 13(12): 4118–4125. https://doi.org/10.1021/bm301378n
25. Naderi A, Lindström T, Sundström J (2014a) Carboxymethylated nanofibrillated cellulose: rheological studies. Cellulose 21:1561–1571. https://doi.org/10.1007/s10570-014-0192-8
26. Naderi A, Lindström T, Pettersson T (2014b) The state of carboxymethylated nanofibrils after homogenization-aided dilution from concentrated suspensions: a rheological perspective. Cellulose 21:2357–2368. https://doi.org/10.1007/s10570-014-0329-9
27. Naderi A, Lindström T, Sundström J, Flodberg G, Erlandsson J (2016a) A comparative study of the properties of three nanofibrillated cellulose systems that have been produced at about the same energy consumption levels in the mechanical delamination step. Nord. Pulp Paper Res. J., 31:364–371. https://doi.org/10.3183/npprj-2016-31-03-p364-371
28. Naderi A, Lindström T (2016b) A comparative study of the rheological properties of three different nanofibrillated cellulose systems. Nord. Pulp Paper Res. J., 31:354–363. https://doi.org/10.3183/npprj-2016-31-03-p354-363
29. Naderi A, Koschella A, Heinze T, Shih KC, Nieh MP, Pfeifer A, Chang CC, Erlandsson J (2017) Sulfoethylated nanofibrillated cellulose: Production and properties. Carbohydr. Polym. 169:515–523. https://doi.org/10.1016/j.carbpol.2017.04.026
30. Nordenström M, Fall A, Nyström G, Wågberg L (2017) Formation of Colloidal Nanocellulose Glasses and Gels. Langmuir, 33:9772–9780. https://doi.org/10.1021/acs.langmuir.7b01832
31. Pääkkö M, Ankerfors M, Kosonen H, Nykänen A, Ahola S, Österberg M, Ruokolainen J, Laine J, Larsson PT, Ikkala O, Lindström T (2007) Enzymatic hydrolysis combined with mechanical shearing and high-pressure homogenization for nanoscale cellulose fibrils and strong gels. Biomacromolecules 8:1934–1941. https://doi.org/10.1021/bm061215p
32. Rantanen J, Maloney TC (2015) Consolidation and dewatering of a microfibrillated cellulose fiber composite paper in wet pressing. Eur Polym J 68:585–591. https://doi.org/10.1016/j.eurpolymj.2015.03.045
33. Saito T, Uematsu T, Kimura S, Enomae T, Isogai A (2011) Self-aligned integration of native cellulose nanofibrils towards producing bulk materials, Soft Matter 7:8804–8809. https://doi.org/10.1039/C1SM06050C
34. Schnell U, Jensen P (2007) Determination of maximum freeze drying temperature for PEG-impregnated archaeological wood. Stud. Conserv. 52: 50–58.

35. Unbehend JE, Britt KW (1982) Retention, drainage, and sheet consolidation. Ind Eng Chem Prod Res Dev 21: 150–153. https://doi.org/10.1021/i300006a004
36. Wetterling, Jonsson S, Mattson T, Theliander H (2017) The Influence of Ionic Strength on the Electroassisted Filtration of Microcrystalline Cellulose. Ind Eng Chem Res 56:12789–12798. https://doi.org/10.1021/acs.iecr.7b03575
37. Wetterling J, Sahlin K, Mattsson T, Westman G, Theliander H (2018) Electroosmotic dewatering of cellulose nanocrystals. Cellulose 25:2321–2329. https://doi.org/10.1007/s10570-018-1733-3
38. Wågberg L, Decher G, Norgren M, Lindström T, Ankerfors M, Axnäs K (2008) The Build-Up of Polyelectrolyte Multilayers of Microfibrillated Cellulose and Cationic Polyelectrolytes. Langmuir 24:784–795. https://doi.org/10.1021/la702481v
39. Yang W, Zhang Y, Liu T, Huang R, Chai S, Chen F, Fu Q (2017) Completely Green Approach for the Preparation of Strong and Highly Conductive Graphene Composite Film by Using Nanocellulose as Dispersing Agent and Mechanical Compression. ACS Sustain. Chem. Eng. 5:9102–9113. https://doi.org/10.1021/acssuschemeng.7b02012
40. Zhu H, Yang X, Cranston E D, Zhu S (2016) Flexible and Porous Nanocellulose Aerogels with High Loadings of Metal-Organic Framework Particles for Separations Applications. Adv Mater, 28: 7652–7657. https://doi.org/10.1002/adma.201601351

Figures

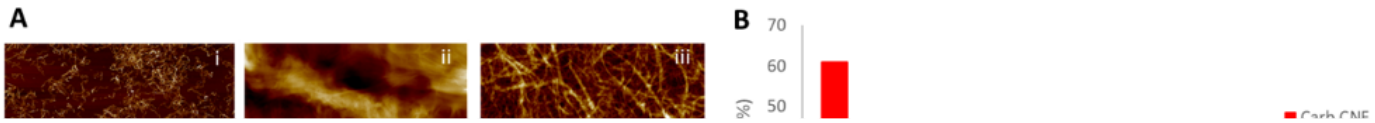

Figure 1

(A) AFM height images for Carb CNF (left, i), Enz CNF (middle, ii), and Ind CNF (right, iii). (B) Nanofraction, (C) Transmittance at 500 nm (C), and Viscosity at 1 s^{-1} (D). Red bars show Carb CNF, blue Enz CNF and black Ind CNF. DI refers to deionized water, and 10mM and 100mM refers to the suspensions NaCl concentration.

Figure 2

Removed water as a function of dewatering time for the pure CNF suspensions and at pH 3 (A). Dewatering rate for the different CNF qualities at the different chemical conditions (B). The dewatering rate is calculated as the slope between 10 and 30 % removed water.

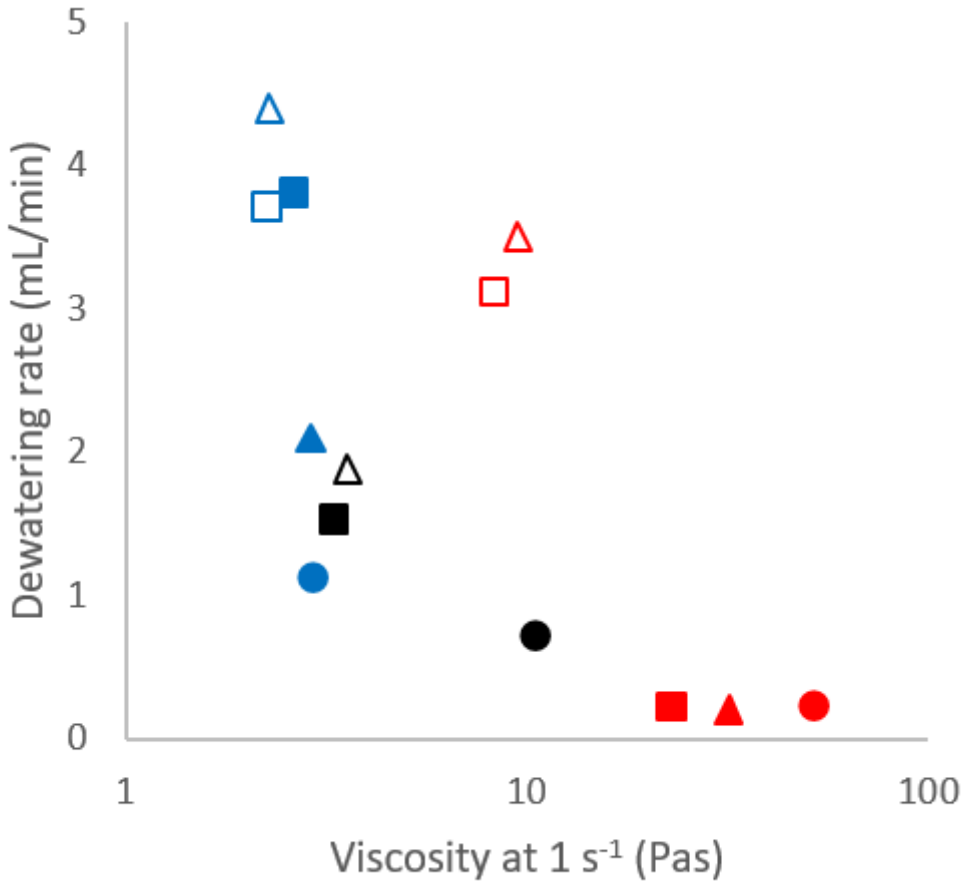

Figure 3

The relation between viscosity and dewatering rate. Red marks show Carb CNF, blue Enz CNF and black Ind CNF. Filled circles reflect the original suspensions. Squares illustrate NaCl additions (filled 10mM and open 100mM), and triangles illustrate pH adjustments (filled pH 5 and open pH 3)

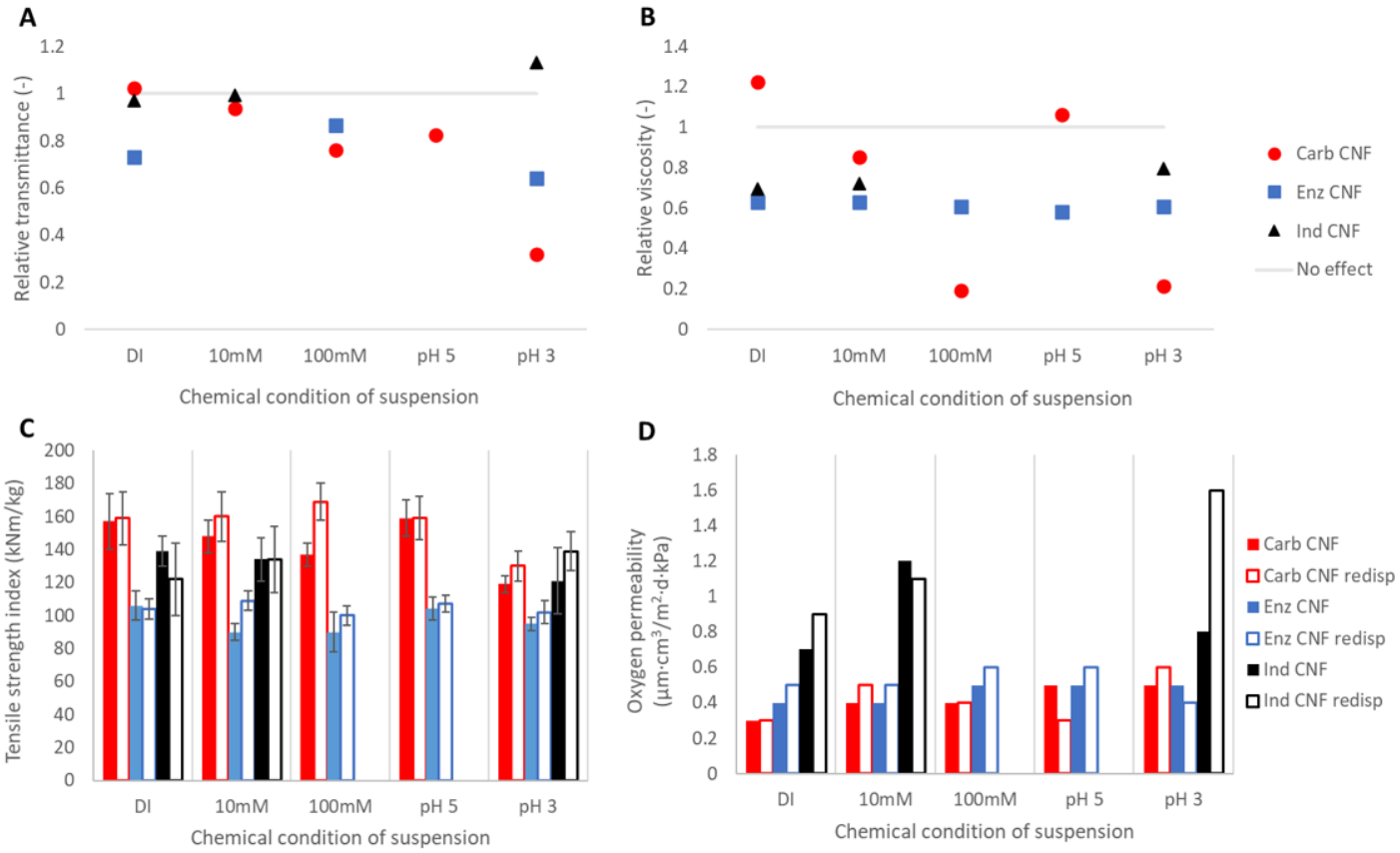

Figure 4

Relative changes in transmittance (A) and viscosity (B) after dewatering and redispersion. Tensile strength index (C) and oxygen permeability (D) for films prepared with the different CNF systems before and after dewatering and redispersion.

Supplementary Files

This is a list of supplementary files associated with this preprint. Click to download.

- FigurTOCred002.pdf